

1 **Ethanolamine regulates CqsR quorum-sensing signaling in *Vibrio cholerae***

2 Samit Watve<sup>1</sup>, Kelsey Barrasso<sup>1,2</sup>, Sarah A. Jung<sup>1,2</sup>, Kristen J. Davis<sup>1,2</sup>, Lisa A. Hawver<sup>1</sup>, Atul

3 Khataokar<sup>3</sup>, Ryan G. Palaganas<sup>4</sup>, Matthew B. Neiditch<sup>3</sup>, Lark J. Perez<sup>4</sup>, Wai-Leung Ng<sup>1,2,#</sup>

4

5 1. Department of Molecular Biology and Microbiology, Tufts University School of Medicine

6 2. Graduate Program in Molecular Microbiology, Tufts Sackler School of Biomedical Sciences

7 3. Department of Microbiology, Biochemistry, and Molecular Genetics, New Jersey Medical

8 School, Rutgers, The State University of New Jersey

9 4. Department of Chemistry & Biochemistry, Rowan University

10 # Corresponding author

11

12 Running Title: Ethanolamine regulates *Vibrio cholerae* quorum sensing

13 Key Words: Signal Transduction, Two-Component Systems, metabolite sensing

14

15

16

17 **ABSTRACT**

18 The pathogen that causes cholera, *Vibrio cholerae*, uses the cell-cell communication process  
19 known as quorum sensing (QS) to regulate virulence factor production and biofilm formation in  
20 response to changes in population density and complexity. QS is mediated through the detection  
21 of extracellular chemical signals called autoinducers. Four histidine kinases, LuxPQ, CqsS, CqsR  
22 and VpsS, have been identified as receptors to activate the key QS regulator LuxO at low cell  
23 density. At high cell density, detection of autoinducers by these receptors leads to deactivation of  
24 LuxO, resulting in population-wide gene expression changes. While the cognate autoinducers that  
25 regulate the activity of CqsS and LuxQ are known, the signals that regulate CqsR have not been  
26 determined. Here we show that the common metabolite ethanolamine specifically interacts with  
27 the ligand-binding CACHE domain of CqsR *in vitro* and induces the high cell-density QS response  
28 through CqsR kinase inhibition in *V. cholerae* cells. We also identified residues in the CqsR  
29 CACHE domain important for ethanolamine detection and signal transduction. Moreover,  
30 mutations disrupting endogenous ethanolamine production in *V. cholerae* delay the onset of, but  
31 do not abolish, the high cell-density QS gene expression. Finally, we demonstrate that modulation  
32 of CqsR QS response by ethanolamine occurs inside animal hosts. Our findings suggest that *V.*  
33 *cholerae* uses CqsR as a dual-function receptor to integrate information from the self-made signals  
34 as well as exogenous ethanolamine as an environmental cue to modulate QS response.

35 **IMPORTANCE**

36 Many bacteria use quorum sensing to regulate cellular processes that are important for their  
37 survival and adaptation to different environments. Quorum sensing usually depends on the  
38 detection on chemical signals called autoinducers made endogenously by the bacteria. We show  
39 here ethanolamine, a common metabolite made by various bacteria and eukaryotes, can modulate  
40 the activity of one of the quorum-sensing receptors in *Vibrio cholerae*, the etiological agent of the  
41 disease cholera. Our results raise the possibility that *V. cholerae* or other quorum-sensing bacteria  
42 can combine environmental sensing and quorum sensing to control group behaviors.

43

## 44 INTRODUCTION

45 Quorum sensing (QS) is used by a wide variety of bacteria to coordinate population-wide  
46 changes in behaviors in response to cell density (1). *Vibrio cholerae*, which causes the diarrheal  
47 disease cholera in the human host, uses QS to regulate virulence factor production, biofilm  
48 formation, Type VI secretion, metabolic regulation, and natural competence to maintain  
49 competitive fitness in various environments (2-10). Four parallel QS signaling systems pathways  
50 have been identified in *V. cholerae* that rely on a phosphorelay to regulate downstream gene  
51 expression (11) (Figure 1). At low cell-density (LCD), four histidine kinases CqsS, LuxPQ, CqsR,  
52 and VpsS function in parallel to phosphorylate LuxO through an intermediate phosphotransfer  
53 protein LuxU (10, 11). Phosphorylated LuxO promotes the transcription of small RNAs Qrr1-4  
54 which promote the translation of the transcriptional regulator AphA (12, 13). Conversely, Qrr1-4  
55 repress the translation of transcriptional regulator HapR (14, 15). Virulence and biofilm genes are  
56 expressed at LCD (4-6, 9, 11). At high cell-density (HCD), each receptor kinase detects its unique  
57 chemical messenger called autoinducer (AI) that inhibits the kinase activity upon signal binding  
58 (1). Autoinducer synthase CqsA catalyzes the production of CAI-1 (*S*-3-hydroxytridecan-4-one)  
59 which is detected by receptor CqsS (16-20) and autoinducer synthase LuxS produces AI-2 (*S*-  
60 TMHF-borate) which is detected by LuxP/Q (21-25). Thus, at HCD, when these receptors are  
61 bound to their cognate signals, kinase activity is inhibited, leading to dephosphorylation of LuxO.  
62 This prevents the transcription of Qrr 1-4 thereby inhibiting AphA production and promoting  
63 HapR translation. Type VI secretion and competence genes are expressed at HCD (3, 7). Another  
64 QS circuit was recently identified in *V. cholerae*, consisting of a cytoplasmic receptor VqmA  
65 which recognizes DPO (3,5-dimethylpyrazin-2-ol) but this system does not participate in  
66 regulating LuxO (26).

67           Although the kinase activity of both CqsR and VpsS is cell-density dependent, the signals  
68   that control the activity of CqsR and VpsS are unclear (11). VpsS has no predicted transmembrane  
69   domains and is thought to be cytoplasmic. Nitric oxide (NO) has been shown to regulate the kinase  
70   activity of VpsS *in vitro* through a signaling partner VpsV (27). However, *V. cholerae* does not  
71   make NO and  $\Delta vpsV$  mutants has no detectable change in QS response (10, 11), so the exact role  
72   of NO sensing by VpsV in *V. cholerae* QS response remains unknown.

73           In contrast, CqsR is predicted to have a periplasmic CACHE domain that is known to be  
74   involved in signal sensing in many chemotaxis receptors (28). Here, by isolating constitutively  
75   active CqsR mutants, we identified several key residues within the CqsR CACHE domain required  
76   for signal binding or signal transduction. Through a chemical library screen and structure-activity  
77   relationship *in vitro* binding assay, we discovered that ethanolamine and its analogs, alaninol and  
78   serinol, bind to the CqsR CACHE domain and modulate QS response of *V. cholerae* through CqsR.  
79   We also determined that *V. cholerae* strains defective in ethanolamine biosynthesis delayed the  
80   onset of, but did not abolish, the HCD QS response. Using an infant mouse colonization model,  
81   we show that ethanolamine modulates *V. cholerae* QS response through CqsR inside animal hosts.  
82   We therefore predict that ethanolamine is used as an external cue for niche sensing and additional  
83   signals are produced by *V. cholerae* to modulate QS through CqsR.

## 84   **MATERIALS AND METHODS**

### 85   **Bioinformatics**

86   Conserved domain structures of *V. cholerae* CqsR (accession no.: NP\_231465.1) were analyzed  
87   using a suite of online tools including CDD (29), CDART (30), InterPro (31), and TMHMM (32).

88 3D structural modelling of the CqsR ligand-binding domain was performed using HHPred (33)  
89 and Phyre2 (34) and compared to the known structure of the periplasmic region of Mlp37 (PDB  
90 ID: 3C8C) (35).

### 91 **Strains, media and culture conditions**

92 All *V. cholerae* strains used in this study were derived from C6706*str2*, a streptomycin-resistant  
93 isolate of C6706 (O1 El Tor) (36). The HapR-dependent bioluminescent reporter pBB1 has been  
94 previously described (11). *V. cholerae* and *E. coli* cultures were grown with aeration in Luria-  
95 Bertani (LB) broth at 30°C and 37°C, respectively. Unless specified, media was supplemented  
96 with streptomycin (Sm, 100 µg/ml), tetracycline (Tet, 5 µg/ml), ampicillin (Amp, 100 µg/ml),  
97 kanamycin (Kan, 100 µg/ml), chloramphenicol (Cm, 5 µg/ml) and polymyxin B (Pb, 50 U/ml)  
98 when appropriate. Bacterial strains used in this study is provided in Supplementary Table 1.

### 99 **DNA manipulations and strain construction**

100 All DNA manipulations were performed using standard procedures. Deletions and point mutations  
101 were introduced into the *V. cholerae* genome by allelic exchange using the suicide vector pKAS32  
102 or a modified version, pJT961, as previously described (11, 37, 38). Mutant strains carrying the  
103 desired mutations were screened and confirmed by PCR and sequencing.

### 104 **Bioluminescence assays**

105 Bioluminescence assays were performed as described previously (11) with slight modifications.  
106 For manual assays, single colonies were grown overnight at 30 °C in LB containing appropriate  
107 antibiotics and the cultures were diluted at least 100-fold in the same medium. Diluted cultures

108 were grown at 30 °C and OD<sub>600</sub> (1 ml of culture) and light production (0.2 ml of culture) were  
109 measured every 45–60 min until OD<sub>600</sub> reached ~2.0 using a Thermo Scientific Evolution 201 UV-  
110 Visible Spectrophotometer and a BioTek Synergy HT Plate Reader, respectively. For automated  
111 assays, single colonies were grown in LB medium containing appropriate antibiotics in 96- or 384-  
112 well microplates at 30°C with aeration. OD<sub>600</sub> and light production were measured every 30 min  
113 for at least 10 hr using a BioTek Synergy HT Plate Reader. Light production per cell was calculated  
114 from dividing light production by OD<sub>600</sub>.

### 115 **Random mutagenesis and screening of constitutively active CqsR mutants.**

116 The region encoding the predicted ligand-binding domain of CqsR (amino acids 31-297) was  
117 amplified from pEVS143-*cqsR* (11, 39) with primers WNTTP0548  
118 (GAGTTATTGGGGGCTTGAAGT) and WNTTP0549  
119 (AATCCTTTTTCGATGTTGATAATTAAGTCG) and subjected to random mutagenesis using  
120 GeneMorph II EZClone Mutagenesis kit (Agilent Technologies) per manufacturer's instructions.  
121 The resulting *cqsR* random mutagenized library was transformed into XL10-Gold *E. coli* cells. A  
122 portion of the library was then conjugated into a quadruple QS receptor strain ( $\Delta 4$ ,  $\Delta cqsS$ ,  $\Delta luxQ$ ,  
123  $\Delta cqsR$ ,  $\Delta vpsS$ ) carrying a HapR-dependent bioluminescence reporter pBB1 (11) and the  
124 transconjugants were selected on LB/Pb/Kan/Tet2 plates and used for screening of constitutively  
125 active CqsR mutants. Colonies were picked and transferred into microplates containing  
126 LB/Kan/Tet2/IPTG medium using a colony picking robot and grown at 30°C overnight. OD<sub>600</sub> and  
127 luminescence were measured with a BioTek Synergy HT Plate Reader. Mutants of interest that  
128 displayed low relative bioluminescence were collected, re-screened again to confirm. The  
129 mutations in the plasmid-borne *cqsR* of these isolates were determined by sequencing. To

130 introduce specific amino acid changes, site directed mutagenesis on the plasmid-borne *cqsR* was  
131 performed using the QuikChange™ XL Site-Directed Mutagenesis Kit (Agilent) per  
132 manufacturer's instructions.

### 133 **NMR metabolomics.**

134 Extracellular metabolite analysis of *V. cholerae* culture supernatants was performed as described  
135 previously (8) except plain LB medium was used as reference standard. An <sup>1</sup>H NMR spectrum of  
136 each sample was collected at 25°C on a Bruker Avance 600 spectrometer by using 64 scans and a  
137 NOE1D pulse sequence. Data were processed and analyzed by using CHENOMX (version 8.0)  
138 for quantification of metabolites present in each sample. The average value and the standard error  
139 of the mean (SEM) were determined for at least three replicates.

### 140 **CqsR LBD purification**

141 The region encoding the periplasmic region of CqsR (CqsR-LBD, residues 35-274) was PCR  
142 amplified with primers WNTP0694  
143 (GCCTGGTGCCGCGCGGCAGCGAAGTCCCATTAGAAAAGAG) and WNTP695  
144 (GCTTTGTTAGCAGCCGGATCTTAGATGTTGATAATTAAGTCGAAG) from *V. cholerae*  
145 genomic DNA; the vector pET28B was amplified with primers WNTP692  
146 (GCTGCCGCGCGGCACCAG) and WNTP693 (GATCCGGCTGCTAACAAAG). The two  
147 fragments were joined together using Gibson reaction (NEB) and the resulting plasmid was  
148 transformed into *E. coli* BL21(DE3) strain (WN5327).

149 For CqsR-LBD purification, strain WN5327 was grown to OD<sub>600</sub> ~ 0.5 and induced with 1 mM  
150 IPTG at 16 °C overnight. Cells were collected by centrifugation and resuspended in binding buffer  
151 (50mM sodium phosphate buffer, pH 7.0; 300mM sodium chloride; 10mM imidazole, pH 7.7; 5%



152 glycerol). Resuspended cells were then lysed with a fluidizer. Insoluble materials were removed  
153 by centrifugation (10,000g, 4 °C, 1 hour) and subsequent filtering through a 0.45 µm filter. Cleared  
154 lysate was loaded onto His-Trap column (1 mL) equilibrated with binding buffer. The column was  
155 then washed with 20 mL binding buffer. Proteins were eluted with binding buffer containing 120  
156 to 300 mM imidazole. Fractions containing CqsR-LBD were pooled, frozen in aliquots, and stored  
157 at -80°C.

### 158 **Differential scanning fluorimetry**

159 Differential scanning fluorimetry assays were performed using a BioRad CFX Connect Real-Time  
160 PCR instrument (40). For chemical screening, ligands were prepared by dissolving the contents of  
161 Biolog plates PM 1-4 in 50 µl of water (final concentration ~10–20 mM). Each 20 µl standard assay  
162 contained 1× PBS (pH 7.5), 10%(v/v) glycerol, 10 µM CqsR-LBD, and 5× SYPRO Orange. Two  
163 µl of the resuspended Biolog compounds were added to each assay. Samples were heat denatured  
164 from 20°C to 90°C at a ramp rate of 1°C min<sup>-1</sup>. The protein unfolding curves were monitored by  
165 detecting changes in SYPRO Orange fluorescence. The first derivative values (-dF/dt) from the  
166 raw fluorescence data were used to determine the melting temperature (T<sub>m</sub>). For testing other  
167 compounds, a 10× stock was prepared and 2 µl was added to each well and the experiments were  
168 conducted as described above.

### 169 **MicroScale Thermophoresis (MST)**

170 Nickel affinity resin-purified CqsR-LBD was further purified using anion exchange  
171 chromatography (Source15Q - GE Healthcare) and size exclusion chromatography (S200 – GE  
172 Healthcare). Purified CqsR-LBD was concentrated to 4.3 mg/ml and stored in 50 mM sodium  
173 phosphate, pH 7.7, and 300 mM sodium chloride. CqsR-LBD was diluted to 20 µM and labeled

174 using the Monolith NT Protein Labeling Ki RED-NHS (NanoTemper Technologies). Different  
175 concentrations of ethanolamine were incubated with 20 nM working stock solutions of labeled  
176 protein in the dark for 30 min at 4° C. After incubation, the samples were transferred into standard  
177 treated capillaries (NanoTemper Technologies) and read in a Monolith NT.115 Blue/Red  
178 instrument at room temperature using 20% LED and medium MST power. Binding affinities were  
179 calculated from three experiments.

### 180 **Chemical Synthesis of EA Metabolites**

181 See supplementary information for chemical synthesis of HEGly and HEHEAA.

### 182 **Ethics statement**

183 All animal experiments were done in accordance with NIH guidelines, the Animal Welfare Act,  
184 and US federal law. The infant mouse colonization experimental protocol B-2018-99 was  
185 approved by Tufts University School of Medicine's Institutional Animal Care and Use Committee.  
186 All animals were housed in a centralized and AAALAC-accredited research animal facility that is  
187 fully staffed with trained husbandry, technical, and veterinary personnel in accordance with the  
188 regulations of the Comparative Medicine Services at Tufts University School of Medicine.

### 189 **Infant mouse colonization model**

190 For *V. cholerae* infection, bacterial strains were grown aerobically overnight in LB/Sm at 30°C  
191 and diluted in LB for inoculum. Approximately 10<sup>6</sup> colony forming units (CFUs) in 50 µl were  
192 introduced orogastrically to 3- to 5-day-old CD-1 mice (Charles River Laboratories). Infected  
193 animals were subsequently gavaged with 50µL 10mM ethanolamine (EA) or vehicle (LB) at 2 and  
194 4 hr post-infection. All animals were sacrificed 8 hours after infection and their small intestines  
195 were harvested and homogenized. *V. cholerae* colonized in the small intestine was enumerated by

196 plating serial dilutions of intestinal homogenate on LB/Sm plates. *V. cholerae* colonization of the  
197 small intestine is presented as a single data point per mouse and data are graphed with the median.  
198 Two-tailed unpaired Student's t tests, assuming unequal variances were used for statistical analyses  
199 \*\*P < 0.01.

## 200 **RESULTS**

### 201 **CqsR is predicted to carry a periplasmic CACHE domain**

202 Similar to other hybrid histidine kinases, CqsR possesses a cytoplasmic phosphoacceptor domain  
203 (aa 355 – 421), an HATPase domain (aa 363 – 583) and a C-terminal response regulator domain  
204 (aa 603- 720). Using various bioinformatics tools, the periplasmic region of CqsR is predicted to  
205 carry a periplasmic dCACHE\_1 domain ((28, 41), aa 44-239, simplified as CACHE domain  
206 hereafter) (Figure 2A). The predicted structure contains the characteristic long N-terminal  $\alpha$ -helix  
207 (green), a linker (yellow) that connects this helix to two globular domains (pocket I, red and pocket  
208 II, blue) with a small  $\alpha$ -helical linker between the two pockets (orange), and a C-terminal  $\alpha$ -helix  
209 (purple) that connects the domain to the cytoplasm (Figure 2B), strikingly similar to other CACHE  
210 proteins, such as *V. cholerae* chemoreceptor Mlp37 (35) (Figure 2B). These similarities strongly  
211 suggest that the periplasmic region of CqsR functions as a ligand-binding domain to regulate its  
212 cytoplasmic kinase activity.

213

### 214 **Identification of residues in the CqsR periplasmic region important for signal sensing or** 215 **signal transduction**

216 CqsR kinase activity is inhibited by an uncharacterized activity present in the spent culture media  
217 from *V. cholerae* (11). We therefore hypothesized that CqsR detects a discrete chemical signal  
218 through the periplasmic CACHE domain and predicted that certain mutations in this domain could

219 impair signal sensing and signal transduction. Consequently, these mutations would turn CqsR  
220 into a constitutively active kinase even in the presence of the cognate signals. To identify these  
221 mutations, we constructed a *cqsR* plasmid library in which the whole periplasmic region was  
222 randomly mutagenized. The randomly mutagenized *cqsR* library was then introduced into a  
223 quadruple receptor mutant ( $\Delta 4$ ) *V. cholerae* strain ( $\Delta luxQ$ ,  $\Delta cqsS$ ,  $\Delta vpsS$ ,  $\Delta cqsR$ ) that also harbors  
224 a HapR-dependent bioluminescent reporter cosmid pBB1 (11). While the quadruple receptor  
225 mutant produces light constitutively due to the constant production of HapR, in the presence of a  
226 plasmid-borne wild type (WT) copy of *cqsR*, this strain produces low bioluminescence at low cell-  
227 density (LCD) and subsequently turns on bioluminescence production at high cell-density (HCD)  
228 due to signal detection and kinase inhibition of CqsR (11). Thus, we predicted that clones carrying  
229 plasmids expressing WT *cqsR* or a null *cqsR* allele would appear bright at HCD, while clones  
230 producing CqsR variants insensitive to the presence of cognate signal would appear darker at HCD.  
231 We measured the bioluminescence of ~26,000 clones from this random library and identified 79  
232 candidates impaired for light production at HCD. Most candidates harbored multiple mutations in  
233 the plasmid-borne *cqsR*. There were 23 unique mutations in these candidates. When each unique  
234 mutation was introduced back to *cqsR* individually, only eight unique mutations in *cqsR* resulted  
235 in lower bioluminescence production at HCD (Figure 2C). These *cqsR* mutations caused changes  
236 in the two aspartate residues (D171V and D178V) mapped to pocket I of the predicted ligand  
237 binding domain, two changes in pocket II (L217S and V219E), four changes (R49S, A259V,  
238 H262Y, and L268I) in the two helical regions that either exit or enter the cellular membrane and  
239 are likely not involved in direct ligand interactions. Strikingly, both Asp171 and Asp198 residues  
240 in the pocket I of CqsR are predicted to be in the same positions as the Asp172 and Asp201 residues  
241 respectively, in Mlp37, which have been shown to be critical for binding to amino acid signals

242 (35). Therefore, our results suggest that, similar to Mlp37, CqsR detects its cognate signals through  
243 the periplasmic CACHE domain.

244

#### 245 **Chemical screen identified ethanolamine as a potential CqsR ligand.**

246 Since the periplasmic CACHE domain is critical for the signal sensing, we attempted to identify  
247 potential ligands capable of binding to the putative CqsR ligand-binding domain (CqsR-LBD), by  
248 performing a differential scanning fluorimetry screen using the common metabolites contained  
249 within the Biolog PM1-4 plates. This assay assumed that ligand binding leads to stabilization of  
250 the target protein, resulting in an increase of melting temperature ( $T_m$ ) of the protein, which can  
251 be determined by measuring the dynamics of Sypro Orange fluorescence emission at different  
252 temperatures. In the absence of exogenous metabolites, the average  $T_m$  of the purified CqsR-LBD  
253 was observed to be 46 °C under the test conditions. Out of the ~400 metabolites tested, including  
254 some of the known compounds that bind CACHE domain such as amino acids, carboxylates, and  
255 polyamines, we only observed a shift in the  $T_m$  of >5 °C in the presence of one tested compound,  
256 ethanolamine (or 2-aminoethanol). The shift in  $T_m$  of CqsR in the presence of ethanolamine was  
257 dose-dependent. The largest shift in  $T_m$  of +15 °C was observed for 10 mM ethanolamine (Table  
258 1) with smaller shifts of +9.33 °C, +6°C and +2°C for 1 mM, 100 μM and 10 μM ethanolamine  
259 respectively. To investigate the specificity of the interactions between ethanolamine and the  
260 CqsR-LBD, we determined how chemical modifications to the ligand affected CqsR-LBD binding  
261 (Table 1). Replacing the hydroxyl group of ethanolamine with a thiol, methyl, or carboxyl group  
262 abolished *in vitro* binding to CqsR-LBD, as indicated by the lack of change in the observed  $T_m$  in  
263 the presence of these compounds. Similarly, replacing the amine group with a thiol or methyl

264 group also abolished *in vitro* binding (Table 1). In addition, single or multiple methylations of the  
265 amine group of ethanolamine also abolished binding (Table 1). We therefore concluded that the  
266 presence of both the amine and the hydroxyl groups in ethanolamine are essential for efficient  
267 CqsR-LBD binding. Side-chain substitutions at the carbon atom next to the hydroxyl group  
268 (labelled i in Table 1) also abolished CqsR-LBD binding regardless of the stereochemistry of the  
269 hydroxyl group. However, substitutions on the carbon atom next to the amine group (labelled ii)  
270 appeared to be better tolerated, as indicated by the increase in  $T_m$  observed for L-alaninol and  
271 serinol (Table 1). Interestingly, stereospecificity is critical for binding activity as indicated by  
272 lower shift in  $T_m$  for D-alaninol, a stereo-isomer of L-alaninol, at the same concentration (Table  
273 1).

274 A recent study showed that a specific ethanolamine derivative, N-(2-hydroxyethyl)-2-(2-  
275 hydroxyethylamino) acetamide [HEHEAA], present in commercial preparations of ethanolamine,  
276 is responsible for promotion of *pipA* transcription in *Pseudomonas sp. GM79* in response to plant  
277 exudates (42). We tested eight common compounds that accumulate during chemical synthesis of  
278 ethanolamine including HEHEAA (42, 43) for their ability to bind to CqsR and, in our hands, none  
279 of the compounds tested produced a change in  $T_m$  of the CqsR-LBD in the binding assay  
280 (Supplementary Table 2), suggesting the CqsR response to ethanolamine was not due to these  
281 common contaminants. Finally, using MicroScale Thermophoresis, we determined the binding  
282 affinity ( $K_d$ ) of ethanolamine to CqsR-LBD is  $\sim 0.5 \mu\text{M}$  (Supplementary Figure 1). Collectively,  
283 our data indicate that ethanolamine and some ethanolamine derivatives bind to CqsR-LBD with a  
284 high degree of specificity.

285 **Effect of ethanolamine and its analogs in regulating *V. cholerae* quorum sensing**

286 Since ethanolamine binds to the CqsR-LBD *in vitro*, we postulated that exogenous addition of  
287 ethanolamine might diminish CqsR kinase activity, leading to premature induction of HCD QS  
288 response in *V. cholerae* cells. To test this, we measured the density-dependent bioluminescence  
289 profile of a  $\Delta 3$  *cqsR*<sup>+</sup> ( $\Delta luxQ$ ,  $\Delta cqsS$ ,  $\Delta vpsS$ ) strain that harbors the HapR-dependent  
290 bioluminescent reporter pBB1 in the presence of varying concentrations of exogenously added  
291 ethanolamine. In the absence of ethanolamine, similar to previously reported (11), the  $\Delta 3$  *cqsR*<sup>+</sup>  
292 strain displayed the characteristic U-shaped HapR-dependent bioluminescence profile due to  
293 changes in CqsR kinase activity in different cell densities (Figure 3A). Induction of HCD QS  
294 response by ethanolamine, as observed by increased levels of light production at low cell densities,  
295 was dose-dependent (Figure 3A). In the presence of 10 mM exogenously added ethanolamine, the  
296 strain was constitutively bright at all cell densities when compared to that from the culture in LB  
297 medium without ethanolamine added (Figure 3A). Moreover, lower concentrations (1mM or  
298 0.1mM) of exogenous ethanolamine also induced a higher level of light production in this reporter  
299 strain. Consistent with our model, using a *Pqrr4-lux* reporter (11), we also determined that  
300 ethanolamine repressed *Qrr4* transcription in the  $\Delta 3$  *cqsR*<sup>+</sup> strain (Supplementary Figure 2). Similar  
301 QS-inducing effects were obtained for L-alaninol and serinol (Figure 3B, 3C and Supplementary  
302 Figure 2). Consistent with the observation that D-alaninol did not show any detectable *in vitro*  
303 binding activity to CqsR, 10 mM D-alaninol was inactive in inducing QS gene expression (Table  
304 I, Figure 3D, and Supplementary Figure 2). In addition, ethanolamine did not induce HapR-  
305 dependent bioluminescence in other triple QS receptor mutants where only CqsS, LuxPQ, or VpsS  
306 is present as the sole QS receptor (Supplementary Figure 3), indicating that ethanolamine induces  
307 QS in a CqsR specific manner. Finally, unlike the strain producing WT CqsR, 10 mM of  
308 ethanolamine did not induce constitutive light production in the CqsR<sup>D171V</sup> and CqsR<sup>D198V</sup> CACHE

309 domain mutants (Figure 3E and Figure 3F). Together, our results strongly suggest that  
310 ethanolamine specifically interacts with the CACHE domain of CqsR to inhibit its kinase activity  
311 and modulate QS gene expression in *V. cholerae*.

### 312 **The role of intrinsically produced ethanolamine in QS**

313 We showed above that exogenous ethanolamine inhibits CqsR kinase activity in *V. cholerae*, we  
314 then tested if endogenously made ethanolamine also plays a role in controlling CqsR. In *E. coli*,  
315 ethanolamine is derived from the degradation of glycerol-3-phosphoethanolamine to glycerol-3-  
316 phosphate and ethanolamine (44, 45). This reaction is predicted to be catalyzed by two *V. cholerae*  
317 glycerophosphodiester phosphodiesterases VCA0136 (GlpQ homolog) and VC1554 (UgpQ  
318 homolog). We used <sup>1</sup>H NMR to determine the ethanolamine level in the cell-free supernatants  
319 derived from both the  $\Delta 3\ cqsR^+$  and the  $\Delta 3\ cqsR^+ \Delta vca0136 \Delta vc1554$  strains. We detected ~25  $\mu$ M  
320 ethanolamine in the supernatants harvested from the  $\Delta 3\ cqsR^+$  strain but the level of ethanolamine  
321 was below the detection limit in the supernatants from the  $\Delta 3\ cqsR^+ \Delta vca0136 \Delta vc1554$  strain.

322 After confirming the double phosphodiesterase mutants did not make any ethanolamine, we used  
323 the HapR-dependent bioluminescence pBB1 reporter to measure the QS response of these strains.  
324 We expected the mutant is impaired in expressing the HCD QS response due to the lack of  
325 ethanolamine to repress the CqsR kinase activity. However, the double phosphodiesterase mutant  
326 still exhibited density-dependent U-shaped bioluminescence profile similar to the  $\Delta 3\ cqsR^+$  strain.  
327 Nevertheless, the onset of the transition to HCD bioluminescence production was delayed in the  
328 double phosphodiesterase mutants (Figure 4), suggesting the inhibition of CqsR kinase activity  
329 and HapR production occur at a higher cell density. Consistent with the above results, using a  
330 *Pqrr4-lux* reporter, light production at LCD was higher in the  $\Delta 3\ cqsR^+ \Delta vca0136 \Delta vc1554$  strain



331 when compared to that of the  $\Delta 3$  *cqsR*<sup>+</sup> strain (Supplementary Figure 4), indicating transcription  
332 of Qrr sRNAs is increased in the absence of endogenous ethanolamine production in the double  
333 phosphodiesterase mutants, resulting in a delayed HapR production. It should be noted that, even  
334 in the absence of endogenous ethanolamine production, repression of Qrr transcription and  
335 induction of HapR production still occur, indicating the presence of additional signals inhibiting  
336 CqsR kinase activity at HCD (Figure 4 and Supplementary figure 4). Moreover, addition of 10  
337 mM ethanolamine increased light production in  $\Delta 3$  *cqsR*<sup>+</sup> as well as in the  $\Delta 3$  *cqsR*<sup>+</sup>  $\Delta$ *vca0136*  
338  $\Delta$ *vc1554* carrying the pBB1 HapR-dependent reporters (Figure 4) and decreased light production  
339 in the same strains carrying the *Pqrr4-lux* reporters (Supplementary figure 4), indicating CqsR  
340 sensing is functional in responding to exogenously supplied ethanolamine in these strains.  
341 Together, our results indicate that while endogenously made ethanolamine participates in QS gene  
342 regulation, *V. cholerae* produces additional signals that are capable of activating QS through CqsR.

### 343 **Ethanolamine modulates CqsR QS signaling inside animal hosts**

344 Production of the Toxin-Coregulated Pili, which is critical for *V. cholerae* host colonization, is  
345 repressed by the HCD QS response (5, 6). We previously showed that the  $\Delta 3$  *cqsR*<sup>+</sup> strain, but not  
346 the  $\Delta 4$  strain, can colonize the small intestines of infant mice (11). To determine if exogenous  
347 ethanolamine influences CqsR signaling *in vivo*, we assayed the ability of the  $\Delta 3$  *cqsR*<sup>+</sup> strains to  
348 colonize the host in the presence of exogenous ethanolamine. While the  $\Delta 3$  *cqsR*<sup>+</sup> strain showed a  
349 ~5-fold decrease in mouse small intestine colonization in the presence of ethanolamine compared  
350 to the group given the vehicle control, the  $\Delta 3$  *cqsR*<sup>D171V</sup> strain showed no significant impairment  
351 in the ability to colonize the infant mouse in the presence of ethanolamine (Figure 5). These results  
352 indicate that high levels of ethanolamine in the gut can prematurely induce the HCD QS response

353 in the  $\Delta 3$  *cqsR*<sup>+</sup> strain and decrease colonization. Importantly, the effect of ethanolamine is  
354 dependent on the interaction between the compound and the CACHE domain of the CqsR.

## 355 **DISCUSSION**

356 In this study, we demonstrated that the periplasmic CACHE domain of CqsR QS receptor  
357 is involved in signal sensing; and we also identified a common metabolite ethanolamine as a signal  
358 that regulates the CqsR QS signaling pathway in *V. cholerae*. The periplasmic CACHE domain is  
359 common in many chemotaxis receptors and other membrane bound regulators (28); and CACHE  
360 domain proteins have been shown to interact with a variety of chemical compounds (28, 35, 41,  
361 46-48). While CACHE domain has been shown to interact with quaternary ammonium including  
362 choline (an ethanolamine analog that CqsR does not interact) to control chemotaxis (49, 50), our  
363 study provided an example where a CACHE domain interacts with an amino alcohol (i.e.,  
364 ethanolamine) to regulate QS gene expression. Of note, the CACHE domain of CqsR shares no  
365 homology to that of another ethanolamine-sensing histidine kinase HK17 (EutW) in *Enterococcus*  
366 *faecalis* or the cytoplasmic transcriptional regulator EutR that detects ethanolamine in *Salmonella*  
367 (51, 52).

368 Although ethanolamine binds to CqsR-LBD with sub-micromolar affinity ( $k_d \sim 0.5 \mu\text{M}$ ),  
369 millimolar level of ethanolamine is needed to fully induce the HCD QS response in *V. cholerae*.  
370 This apparent difference is not uncommon for signaling pathways dependent on CACHE receptor  
371 proteins (e.g.,(50, 53)). This is in stark contrast to the typical effective concentration for canonical  
372 autoinducers, such as CAI-1 and AI-2, which are in micromolar levels (16-19, 24, 25).  
373 Nonetheless, interaction of ethanolamine to CqsR is highly specific and modifications of almost  
374 any functional groups in ethanolamine result in total loss of activity. We reasoned that while  
375 ethanolamine binds to CqsR-LBD with high affinity *in vitro*, the binding affinity to the full length

376 CqsR inside *V. cholerae* cells could be different. Moreover, the import mechanism of ethanolamine  
377 into the *V. cholerae* periplasmic space is unclear. Indeed, *V. cholerae* is not known to metabolize  
378 ethanolamine as either carbon or nitrogen source (54) and it lacks the known ethanolamine  
379 transporters for importing the compound into the cytoplasm (55, 56). In addition, since the mutants  
380 defective in ethanolamine synthesis are still able to express a delayed HCD QS response, additional  
381 signals must be present and detected by CqsR, and these molecules could compete with  
382 ethanolamine for CqsR binding.

383         Given *V. cholerae* does not use ethanolamine as a nutrient source, it is unclear why CqsR  
384 detects this specific metabolite out of many secreted molecules. However, ethanolamine has been  
385 implicated in niche recognition in several pathogens such as enterohaemorrhagic *E. coli* (EHEC),  
386 *S. typhimurium* (57), *E. faecalis* (58), and *Clostridium difficile* (59). Our results suggest that  
387 ethanolamine signaling may only operate in environments where ethanolamine is found in high  
388 abundance. Because ethanolamine is derived from the membrane phospholipid turnover, this  
389 compound is particularly prevalent in the gastrointestinal tract, where it can be found at  
390 concentrations over 2 mM per some reports (60). Thus, ethanolamine might act primarily as an  
391 environmental cue as opposed to a *bona fide* QS signal in *V. cholerae*. In *Salmonella*, ethanolamine  
392 metabolism genes and Type 3 secretion system genes are activated with high and low level of  
393 ethanolamine, respectively (57, 61). Similarly, in EHEC, exogenous ethanolamine increases the  
394 expression of virulence genes (51). However, unlike these examples in which ethanolamine  
395 sensing promotes virulence gene expression, ethanolamine detection through CqsR instead  
396 represses virulence gene expression by promoting HCD QS response in *V. cholerae* (11). This is  
397 especially relevant to the life cycle of *V. cholerae* since the major colonization site of this pathogen  
398 is the small intestine while ethanolamine may be more abundant in the lower gastrointestinal (GI)

399 tract because it cannot be metabolized by the majority of commensal species (62), thus,  
400 ethanolamine sensing may prevent *V. cholerae* from colonizing in an undesirable niche.

401 It is puzzling why *V. cholerae* QS circuit is composed of four functionally-redundant  
402 pathways, we previously suggest that the “many-to-one” arrangement is important for the  
403 robustness of the system to prevent signal perturbation and the HCD QS response is only expressed  
404 when all four receptors are bound with the cognate signals (11). Our results here suggest that the  
405 four QS receptors integrate information derived from different sources. It has been suggested CAI-  
406 1 is used for inter-*Vibrio* signaling (16, 18) and AI-2 is for inter-species signaling (63, 64); perhaps  
407 CqsR serves as a dual-function receptor that senses an unknown self-made signal (e.g.,  
408 autoinducer) and an exogenous metabolic by-product as an environmental cue. A combination of  
409 different signals ensures *V. cholerae* only expresses the HCD QS response to repress virulence  
410 factor production and biofilm formation at the most appropriate time and environment. This kind  
411 of dual detection of cognate AIs and other chemical signals by a single QS receptor is not  
412 commonly observed. QseC is one of the known QS receptors that detects both an AI signal (AI-3)  
413 and other chemical cues (epinephrine and norepinephrine) to control virulence gene expression in  
414 *E. coli* and *Salmonella* (69). It is proposed that such unique QS receptor can be used for  
415 communication between the pathogens and the hosts (52). Further work is required to elucidate  
416 the role of ethanolamine sensing in inter-kingdom QS signaling and virulence control in *V.*  
417 *cholerae*.

#### 418 **ACKNOWLEDGEMENTS**

419 We thank James Baleja for assistance with performing NMR metabolomics experiments, and Juan  
420 Hernandez and David Giacalone for technical help. WLN, SW, KB, LAH were supported in part

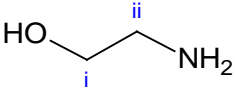
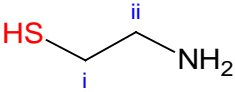
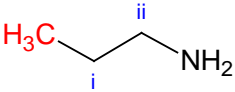
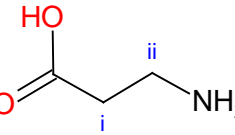
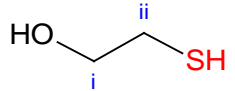
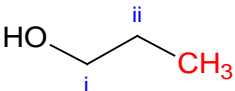
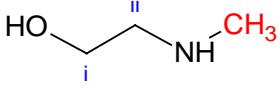
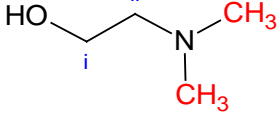
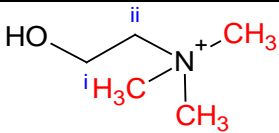
421 by NIH grants AI007329, and AI121337. The funders had no role in study design, data collection  
422 and interpretation, or the decision to submit the work for publication

423

424

425

**TABLE 1 Effects of ethanolamine and its analogs on the melting temp of CqsR-LBD.**

Compound	Structure <sup>a</sup>	T <sub>m</sub> (°C) <sup>b</sup>
None	-	46
Ethanolamine [2-aminoethanol]		61
Cysteamine [2-aminoethanethiol]		46
1-propanamine		46.33 [1.15]
β-alanine [2-Carboxyethylamine]		46
Mercaptoethanol [2-Hydroxyethanethiol]		46
1-Propanol		43.67 [0.58]
2-Methylaminoethanol		49.67 [0.58]
2-Dimethylaminoethanol		48
Choline [(2-Hydroxyethyl)trimethyl ammonium]		46

(S)-(+)-1-Amino-2-propanol		48.67 [0.58]
(R)-(-)-1-Amino-2-propanol		48
L-alaninol [(S)-(+)-2-Amino-1-propanol]		60
D-alaninol [(R)-(-)-2-Amino-1-propanol]		45
Serinol [2-Amino-1,3-propanediol]		53.67 [0.58]

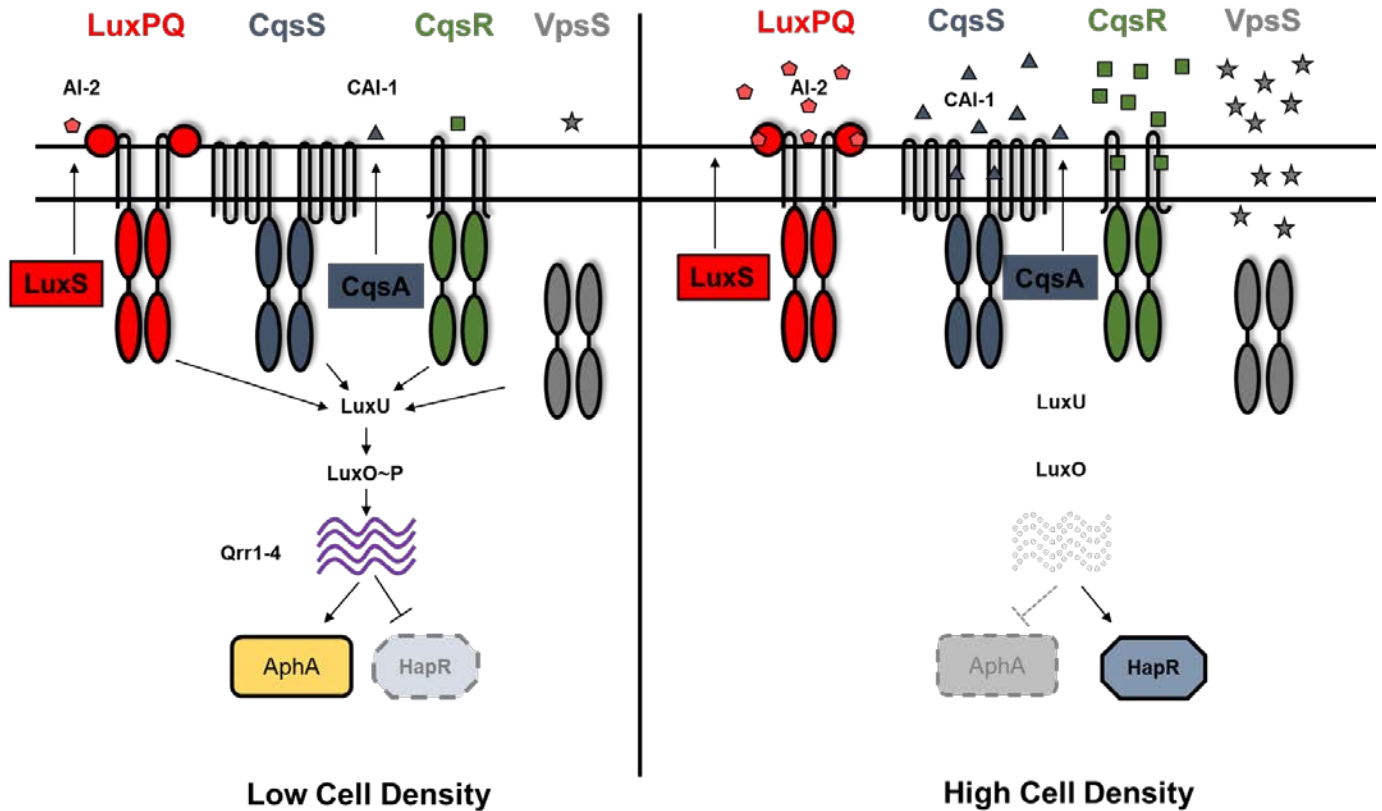
426 <sup>a</sup>Functional groups displayed in red are the ones that vary from the base compound ethanolamine.

427 <sup>b</sup>Data shown as average of 3 replicates in the presence of 10 mM tested compounds. Square

428 brackets indicate standard deviation where applicable.

429

430

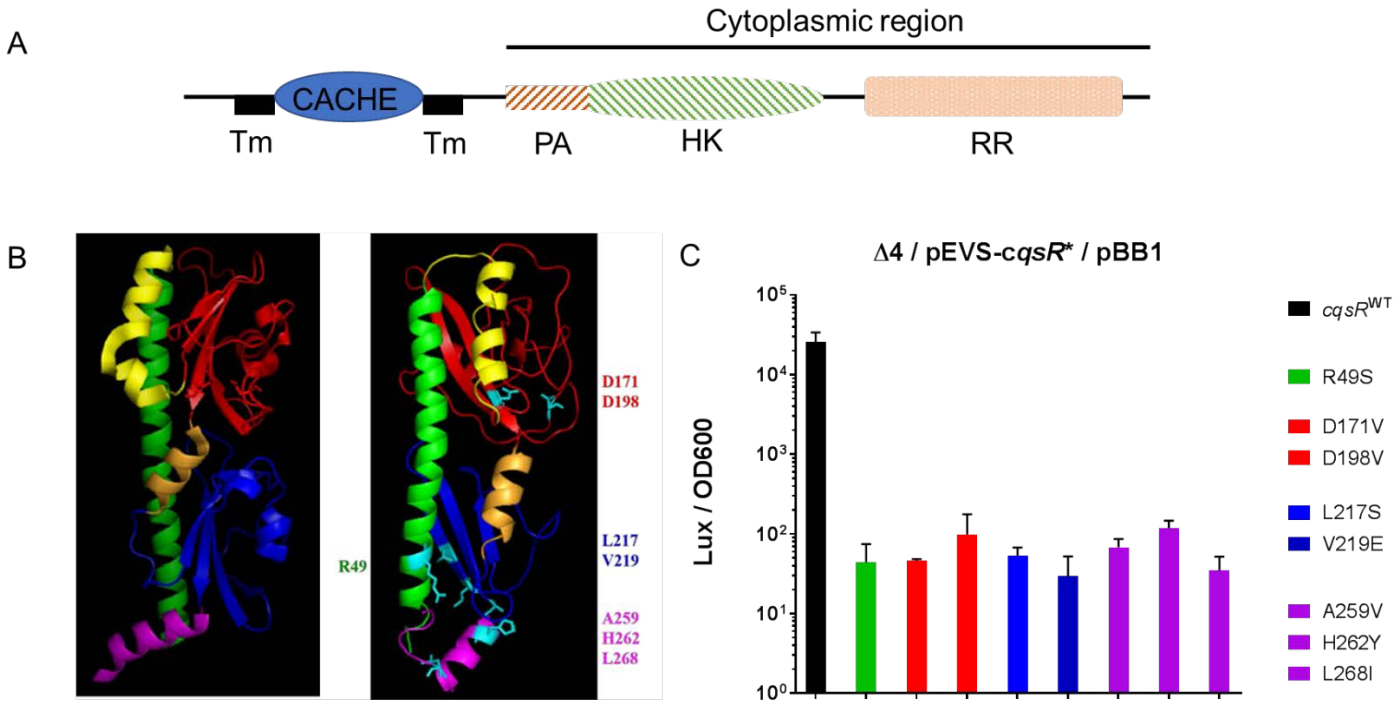


431

432 **Figure 1** Quorum-sensing circuit in *Vibrio cholerae*

433 Quorum sensing in *V. cholerae* is controlled by four histidine kinases CqsS, LuxPQ, CqsR and  
434 VpsS. At low cell density, these receptors act predominantly as kinases and phosphorylate LuxO  
435 through LuxU. Phosphorylated LuxO activates transcription of small RNAs Qrr1-4 which inhibit  
436 HapR translation and promote AphA translation, thereby resulting in a low cell density expression  
437 profile. At high cell density, when the cognate signals are bound, the kinase activity of these  
438 receptors is repressed. This leads to dephosphorylation of LuxO, preventing Qrr1-4 transcription.  
439 Therefore, HapR translation is induced and AphA translation repressed, leading to a high cell  
440 density gene expression pattern. Autoinducers CAI-1 (produced by CqsA) and AI-2 (produced by  
441 LuxS) have been previously characterized in regulating the kinase activity of CqsS and LuxPQ  
442 respectively.





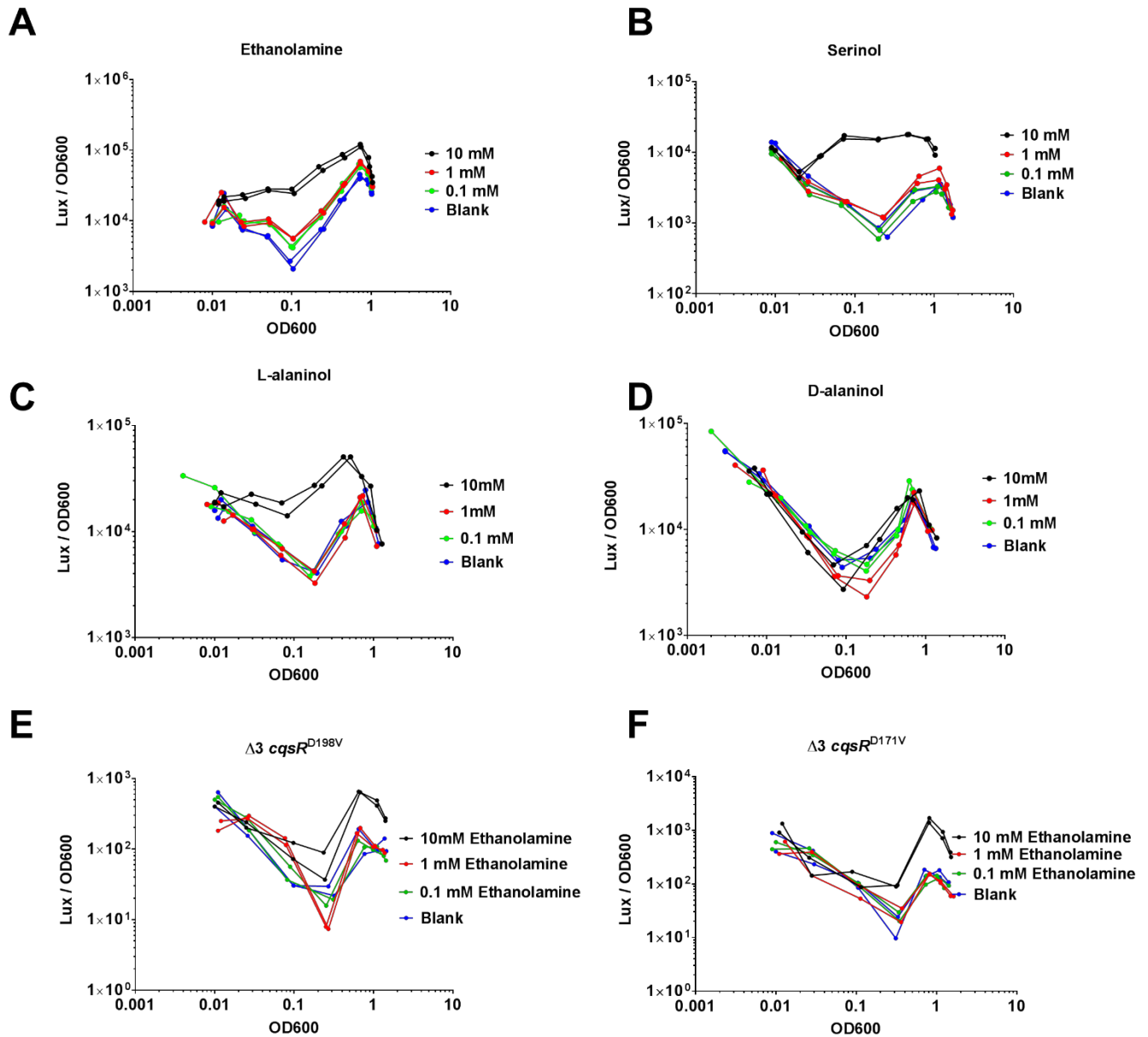
443

444 **Figure 2**

445 **The CqsR CACHE domain is important for signal sensing and signal transduction.**

446 (A) CqsR is predicted to contain all the conserved cytoplasmic domains (phosphoacceptor (PA),  
447 histidine kinase (HK), and response regulator (RR) domains) of a hybrid histidine kinase with an  
448 N-terminal periplasmic CACHE domain flanked by two transmembrane helices (TM). (B) The  
449 predicted structure of the periplasmic CACHE domain of CqsR (right) is similar to that of Mlp37  
450 (left). The residues identified as important for signal sensing and signal transduction are  
451 highlighted in cyan in the predicted structure. See main text for further details. (C) Eight  
452 periplasmic CqsR residues are involved in signal sensing and signal transduction. Relative light  
453 production (lux/OD<sub>600</sub>) was measured in quadruple QS receptor ( $\Delta 4$ ) strains carrying a plasmid  
454 producing CqsR with single amino changes as well as a HapR-dependent bioluminescence  
455 reporter. Alteration in the CqsR helix domain (R49S), CACHE pocket 1 region (D171V, D198V),  
456 CACHE pocket 2 region (L217S, V219E), or the transmembrane proximal regions (A259V,  
457 H262Y, L268I) impaired bioluminescence production at high cell-density (OD<sub>600</sub> > 1.5). Average  
458 values and standard errors from at least three independent replicates are shown.

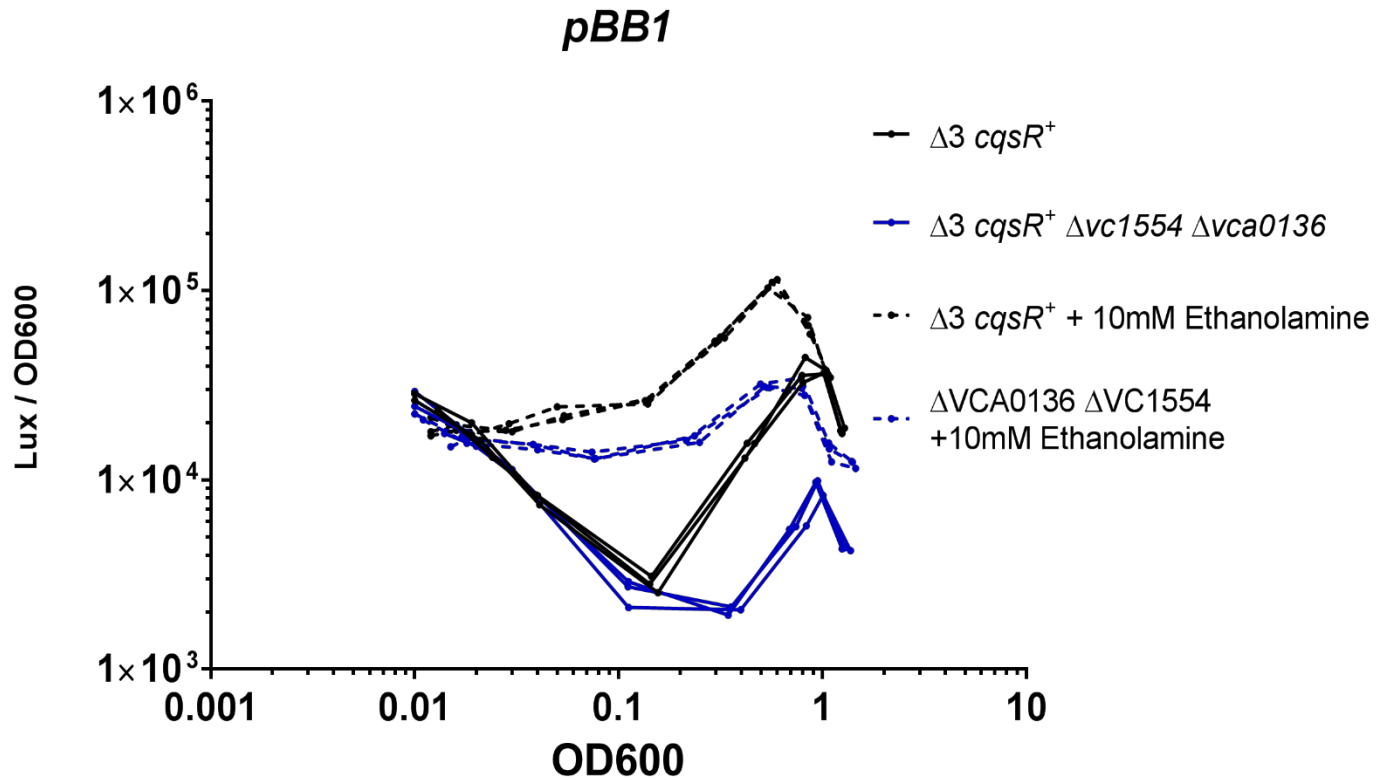
459



460

461 **Figure 3 Effects of ethanolamine and its analogs on CqsR quorum-sensing response.**

462 HapR-dependent bioluminescence profiles (lux/OD<sub>600</sub>) were measured in a  $\Delta 3$  *cqsR*<sup>+</sup> strain in the  
463 presence of 10 mM, 1 mM, 0.1 mM A) ethanolamine, B) serinol, C) L-alaninol, D) D-alaninol.  
464 Blank indicates LB medium without ethanolamine added. HapR-dependent bioluminescence  
465 profiles (lux/OD<sub>600</sub>) were measured in E)  $\Delta 3$  *cqsR*<sup>D198V</sup> strain and F)  $\Delta 3$  *cqsR*<sup>D171V</sup> strain in the  
466 presence of 10 mM, 1 mM, 0.1 mM concentrations ethanolamine respectively. Each figure shows  
467 a representative profile of each condition with two biological replicates. Each experiment was  
468 performed independently at least two times.

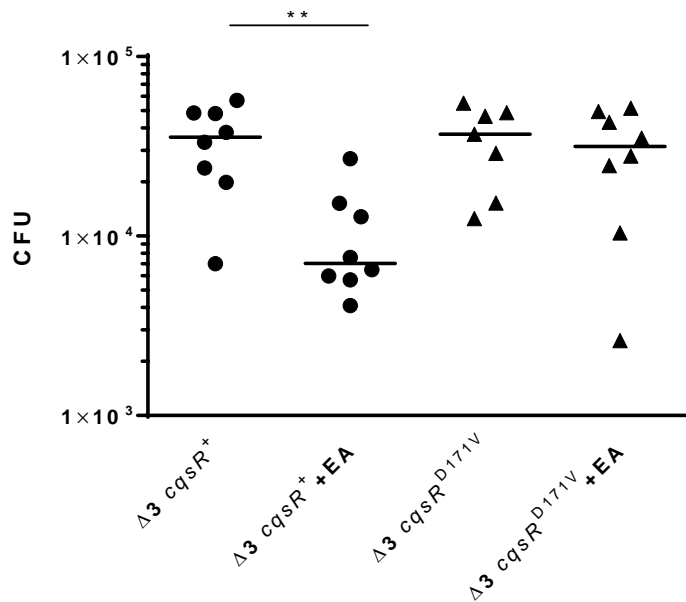


469

470 **Figure 4 Effect of glycerophosphodiesterase deletions on CqsR quorum-sensing response.**

471 HapR-dependent bioluminescence profiles (lux/OD<sub>600</sub>) were measured in a  $\Delta 3 cqsR^+$  strain and an  
472 isogenic strain with deletions in loci *vc1554* and *vca0136*, encoding the two putative  
473 glycerophosphodiester phosphodiesterases in LB medium and in the presence of 10 mM  
474 ethanolamine. The figure shows a representative profile of each condition with two biological  
475 replicates. Each experiment was performed independently at least two times.

476



477

478 **Figure 5 Effect of exogenous ethanolamine on CqsR quorum-sensing response inside animal**

479 **hosts.**

480 CFU counts per small intestine homogenate collected from mice (n = 7-8) infected with a  $\Delta 3$  *cqsR*<sup>+</sup>  
481 or  $\Delta 3$  *cqsR*<sup>D171V</sup> mutant strain. To assess the effect of ethanolamine on strain colonization, mice  
482 were gavaged with 10mM ethanolamine (EA) or vehicle at 2 and 4 hours post infection. Each  
483 symbol represents the CFU enumerated from an individual mouse and the horizontal lines indicate  
484 the median for each group. \*\*P < 0.01 (unpaired t test).

485

486

487 SUPPLEMENTARY INFORMATION

488 Supplementary Table 1. List of strains used in this study

Strain Number	Organism	Genotype	Ab Resistance <sup>a</sup>	Source
WN3176	<i>V. cholerae</i>	$\Delta cqsS \Delta luxQ \Delta vpsS$	Sm	(11)
WN3208	<i>V. cholerae</i>	$\Delta cqsS \Delta luxQ \Delta vpsS / pBB1$	Sm Tet	(11)
WN3357	<i>V. cholerae</i>	$\Delta cqsS \Delta luxQ \Delta cqsR / pBB1$	Sm Tet	(11)
WN3649	<i>V. cholerae</i>	$\Delta cqsS \Delta cqsR \Delta vpsS / pBB1$	Sm Tet	(11)
WN3651	<i>V. cholerae</i>	$\Delta luxQ \Delta cqsR \Delta vpsS / pBB1$	Sm Tet	(11)
WN3354	<i>V. cholerae</i>	$\Delta cqsS \Delta luxQ \Delta vpsS \Delta cqsR$	Sm	(11)
WN4899	<i>V. cholerae</i>	$\Delta cqsS \Delta luxQ \Delta vpsS \Delta cqsR / pEVS143-cqsR / pBB1$	Sm Kan Tet	This study
WN5267	<i>V. cholerae</i>	$\Delta cqsS \Delta luxQ \Delta vpsS \Delta cqsR / pEVS143-cqsR^{R49S} / pBB1$	Sm Kan Tet	This study
WN5275	<i>V. cholerae</i>	$\Delta cqsS \Delta luxQ \Delta vpsS \Delta cqsR / pEVS143-cqsR^{D198V} / pBB1$	Sm Kan Tet	This study
WN5277	<i>V. cholerae</i>	$\Delta cqsS \Delta luxQ \Delta vpsS \Delta cqsR / pEVS143-cqsR^{L217S} / pBB1$	Sm Kan Tet	This study
WN5279	<i>V. cholerae</i>	$\Delta cqsS \Delta luxQ \Delta vpsS \Delta cqsR / pEVS143-cqsR^{V219E} / pBB1$	Sm Kan Tet	This study
WN5281	<i>V. cholerae</i>	$\Delta cqsS \Delta luxQ \Delta vpsS \Delta cqsR / pEVS143-cqsR^{A259V} / pBB1$	Sm Kan Tet	This study
WN5285	<i>V. cholerae</i>	$\Delta cqsS \Delta luxQ \Delta vpsS \Delta cqsR / pEVS143-cqsR^{H262Y} / pBB1$	Sm Kan Tet	This study
WN5318	<i>V. cholerae</i>	$\Delta cqsS \Delta luxQ \Delta vpsS \Delta cqsR / pEVS143-cqsR^{F268I} / pBB1$	Sm Kan Tet	This study
WN5354	<i>V. cholerae</i>	$\Delta cqsS \Delta luxQ \Delta vpsS \Delta cqsR / pEVS143-cqsR^{D171V} / pBB1$	Sm Kan Tet	This study
WN5781	<i>V. cholerae</i>	$\Delta cqsS \Delta luxQ \Delta vpsS \Delta vc1554 \Delta vca0136$	Sm	This study
WN5784	<i>V. cholerae</i>	$\Delta cqsS \Delta luxQ \Delta vpsS \Delta vc1554 \Delta vca0136 / pBB1$	Sm Tet	This study
WN5886	<i>V. cholerae</i>	$\Delta cqsS \Delta luxQ \Delta vpsS cqsR^{D198V}$	Sm	This study
WN5887	<i>V. cholerae</i>	$\Delta cqsS \Delta luxQ \Delta vpsS cqsR^{D171V}$	Sm	This study
WN5890	<i>V. cholerae</i>	$\Delta cqsS \Delta luxQ \Delta vpsS cqsR^{D198V} / pBB1$	Sm Tet	This study
WN5891	<i>V. cholerae</i>	$\Delta cqsS \Delta luxQ \Delta vpsS cqsR^{D171V} / pBB1$	Sm Tet	This study
WN5976	<i>V. cholerae</i>	$\Delta cqsS \Delta luxQ \Delta vpsS / pBK1003 (Pqrr4-lux)$	Sm Cm	This study
WN5979	<i>V. cholerae</i>	$\Delta cqsS \Delta luxQ \Delta vpsS \Delta vc1554 \Delta vca0136 / pBK1003$	Sm Cm	This study
WN5980	<i>V. cholerae</i>	$\Delta cqsS \Delta luxQ \Delta vpsS cqsR^{D198V} / pBK1003$	Sm Cm	This study
WN5981	<i>V. cholerae</i>	$\Delta cqsS \Delta luxQ \Delta vpsS cqsR^{D171V} / pBK1003$	Sm Cm	This study
WN048	<i>E. coli</i>	$S17-1 \lambda pir / pBB1$	Tet	(11)
WN3705	<i>E. coli</i>	$S17-1 \lambda pir / pEVS143-cqsR$	Kan	(11)
WN5233	<i>E. coli</i>	XL10-Gold / $pEVS143-cqsR^{V219E}$	Kan	This study
WN5236	<i>E. coli</i>	XL10-Gold / $pEVS143-cqsR^{A259V}$	Kan	This study
WN5239	<i>E. coli</i>	XL10-Gold / $pEVS143-cqsR^{H262Y}$	Kan	This study

<b>WN5242</b>	<i>E. coli</i>	XL10-Gold / <i>pEVS143-cqsR</i> <sup>R49S</sup>	Kan	This study
<b>WN5248</b>	<i>E. coli</i>	XL10-Gold / <i>pEVS143-cqsR</i> <sup>D198V</sup>	Kan	This study
<b>WN5250</b>	<i>E. coli</i>	XL10-Gold / <i>pEVS143-cqsR</i> <sup>L217S</sup>	Kan	This study
<b>WN5318</b>	<i>E. coli</i>	XL10-Gold / <i>pEVS143-cqsR</i> <sup>F268I</sup>	Kan	This study
<b>WN5326</b>	<i>E. coli</i>	BL21DE3/ pET28b <i>cqsR</i> -LBD	Kan	This study
<b>WN5344</b>	<i>E. coli</i>	XL10-Gold / <i>pEVS143-cqsR</i> <sup>D171V</sup>	Kan	This study
<b>WN5745</b>	<i>E. coli</i>	S17 $\lambda$ pir DAP- / pKAS::Kan <i><math>\Delta</math>vc1554</i>	Kan	This study
<b>WN5746</b>	<i>E. coli</i>	S17 $\lambda$ pir DAP- / pKAS::Kan <i><math>\Delta</math>vca0136</i>	Kan	This study
<b>WN5880</b>	<i>E. coli</i>	S17 $\lambda$ pir DAP- / pKAS::Kan <i>cqsR</i> <sup>D198V</sup>	Kan	This study
<b>WN5881</b>	<i>E. coli</i>	S17 $\lambda$ pir DAP- / pKAS::Kan <i>cqsR</i> <sup>D171V</sup>	Kan	This study

489 <sup>a</sup> Sm = Streptomycin, Kan = Kanamycin, Cm = Chloramphenicol, Tet = Tetracycline

490

491 **Supplementary Table 2**

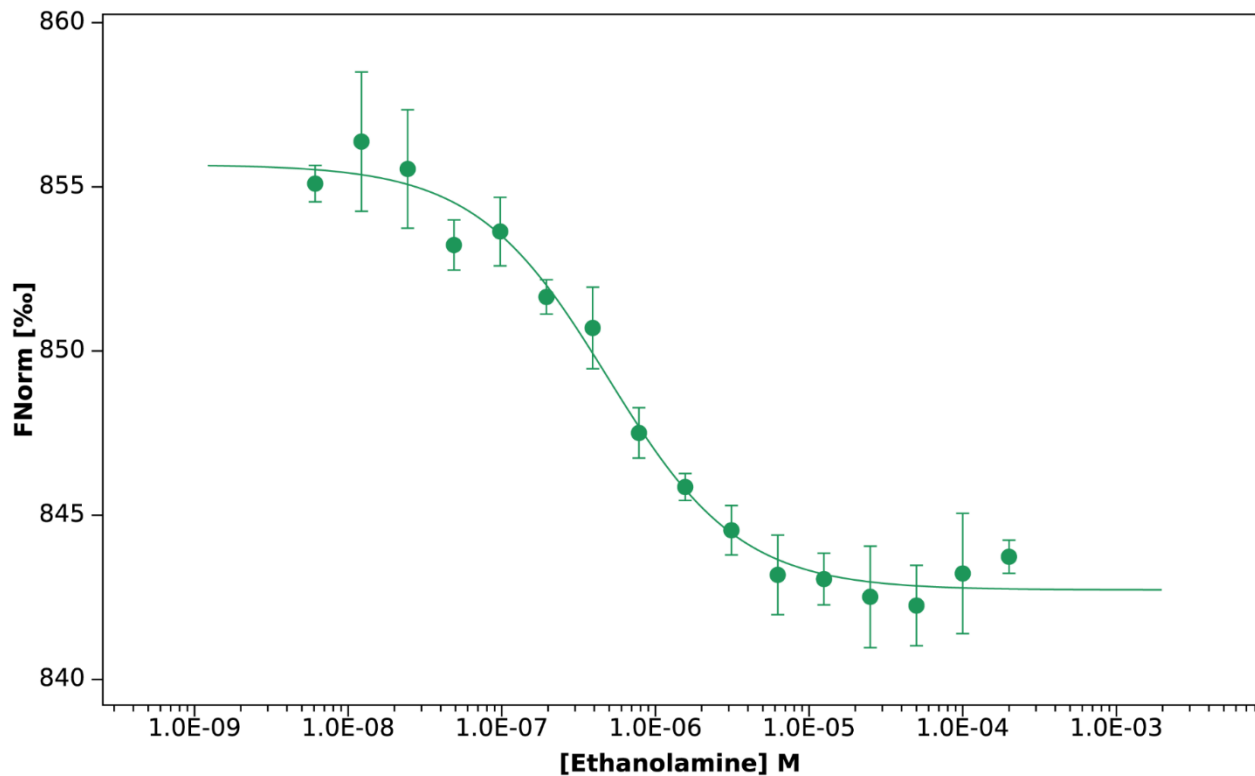
492 **Binding activity of CqsR to common byproducts of ethanolamine**

<b>Compound</b>	<b>T<sub>m</sub><sup>a</sup></b>
None	47.00
N-(2-hydroxyethyl)-acetamide	48.00
N,N'-Bis(2-hydroxyethyl)-ethanediamide	49.00
N-(2-hydroxyethyl)-2-[(2-hydroxyethyl)amino]-acetamide	47.67 [0.57]
N-(2-hydroxyethyl)ethylenediamine	47.67 [0.57]
N-(2-hydroxyethyl)imidazolidone	47.00
N-(2-hydroxyethyl)-glycine	47.33 [0.57]
N-(2-hydroxyethyl)-imidazole	47.33 [0.57]
N-(2-hydroxyethyl)-formamide	50.00

493 <sup>a</sup>Data shown as average of 3 replicates in the presence of 1 mM tested compounds. Square brackets  
494 indicate standard deviation where applicable.

495

496



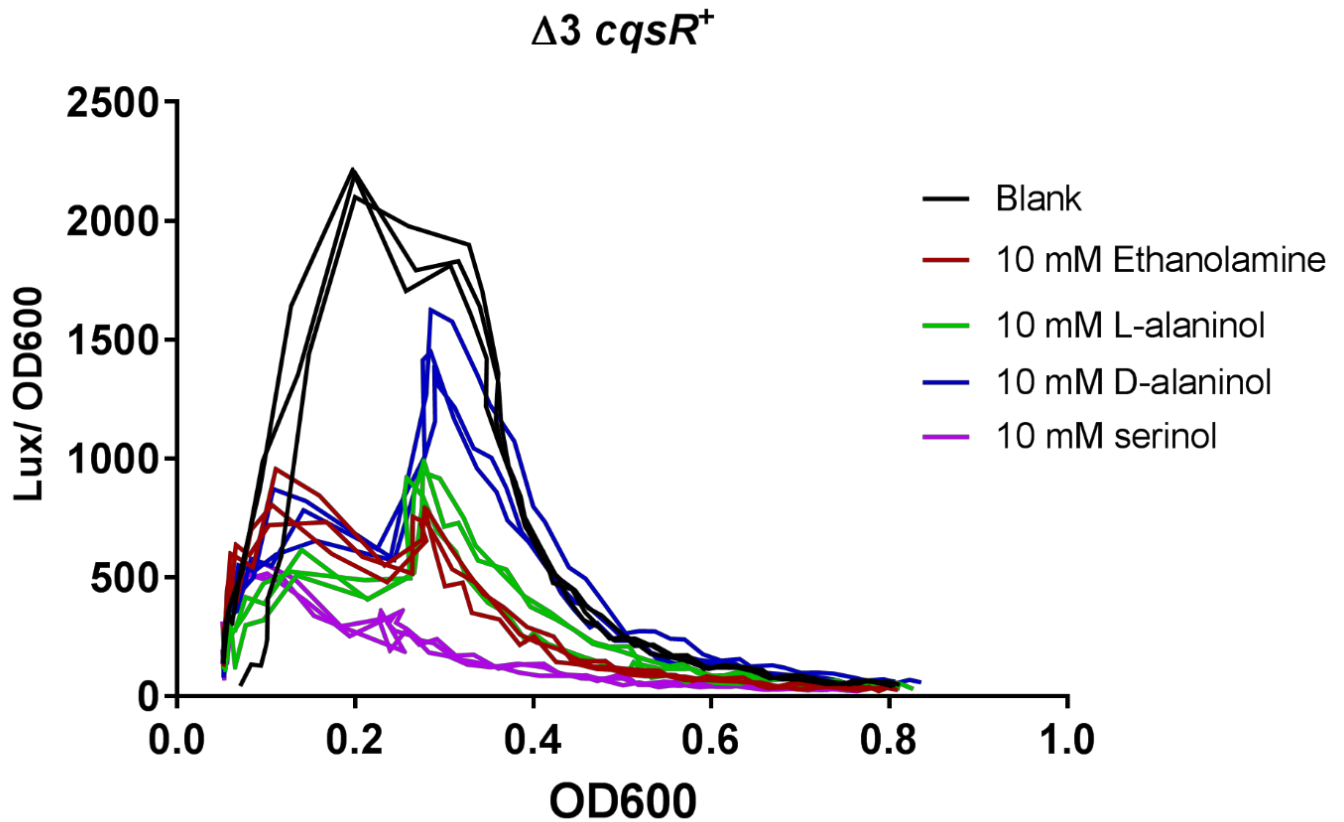
497

### 498 **Supplementary Figure 1**

499 MST quantification (FNorm; normalized fluorescence) for ethanolamine binding to CqsR.  
500 Ethanolamine was titrated between 200  $\mu\text{M}$  and 0.0061  $\mu\text{M}$  with 20 nM His6-tagged CqsR.  
501 Ethanolamine binds to CqsR with a  $K_d$  of  $0.478 \pm 0.076 \mu\text{M}$ . Binding affinity was calculated from  
502 three independent experiments.

503





504

505

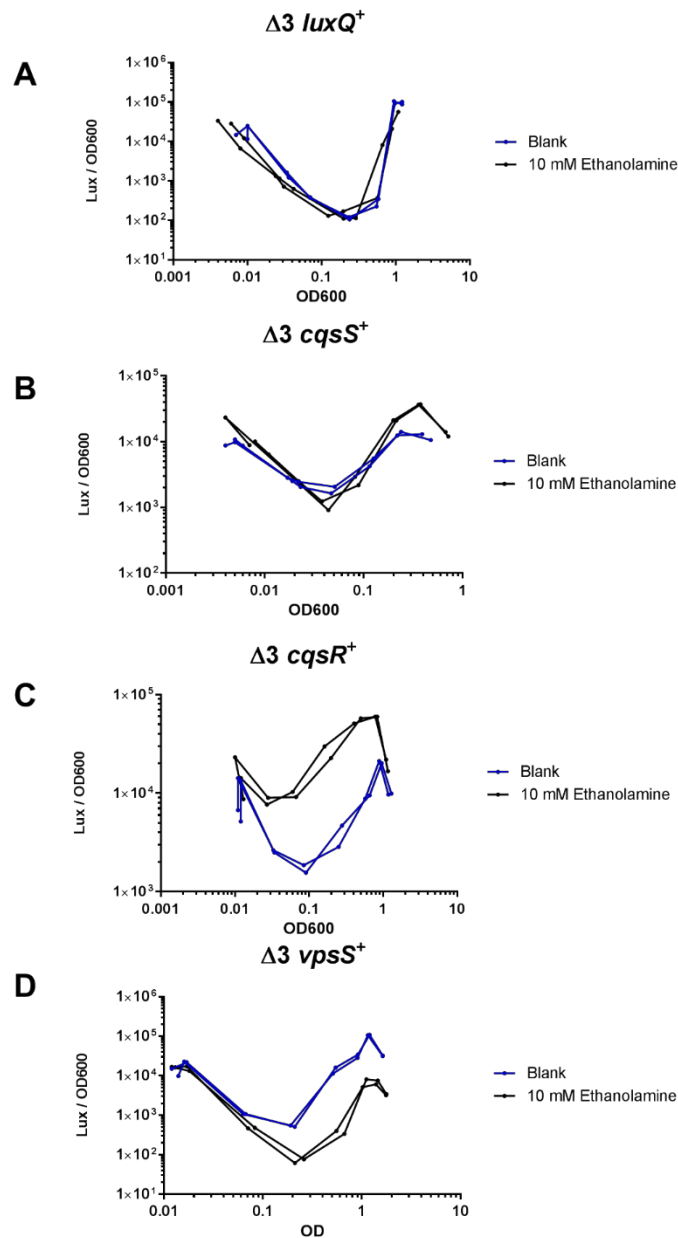
506 **Supplementary Figure 2**

507 **Effect of ethanolamine and its analogs on *qrr4* transcription.**

508 Normalized bioluminescence production (lux/OD<sub>600</sub>) using a *P<sub>qrr4</sub>-lux* reporter was measured in  
509 a  $\Delta 3$  *cqsR*<sup>+</sup> strain in the presence of 10 mM ethanolamine, L-alaninol, D-alaninol, or serinol.  
510 Blank indicates LB medium without added compound.

511

512

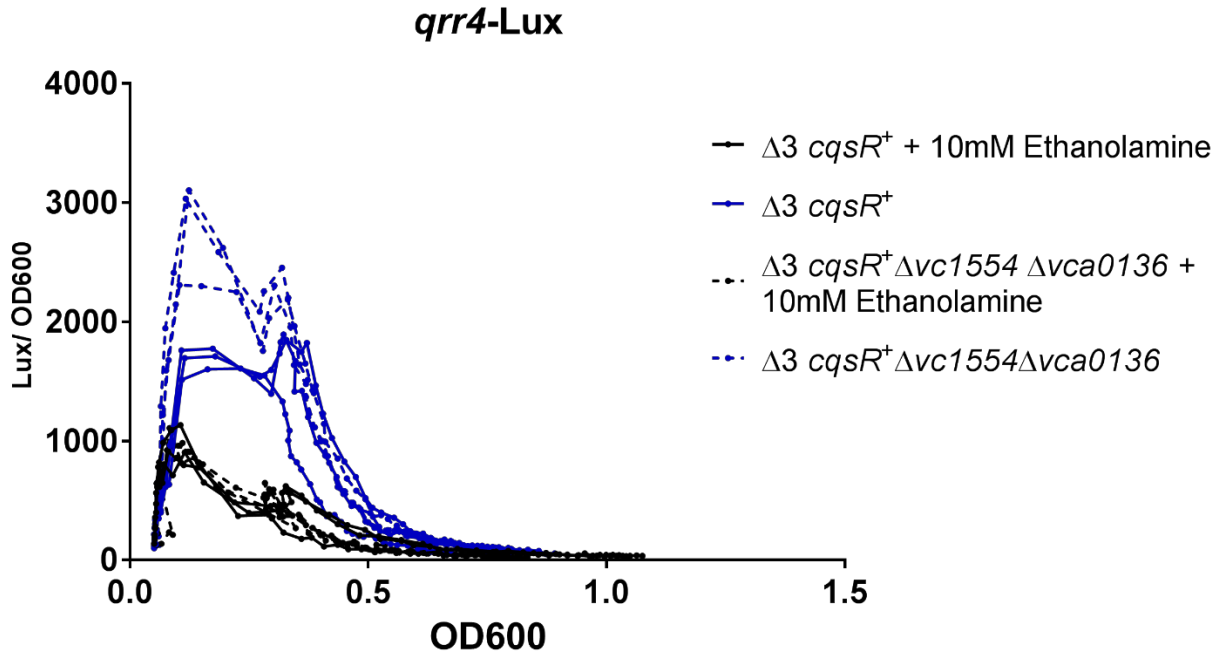


513

### 514 **Supplementary Figure 3**

#### 515 **Ethanolamine induces high cell density QS response in a CqsR-specific manner**

516 HapR-dependent bioluminescence profiles (lux/OD<sub>600</sub>) were measured in A)  $\Delta 3 luxQ^+$ , B)  $\Delta 3$   
517  $cqsS^+$ , C)  $\Delta 3 cqsR^+$ , and D)  $\Delta 3 vpsS^+$ , in LB medium and LB medium containing 10 mM  
518 ethanolamine. Each figure shows a representative profile of each condition with two biological  
519 replicates. Each experiment was performed independently at least two times.



520

521 **Supplementary Figure 4**

522 **Effect of ethanolamine on *qrr4* transcription in the double phosphodiesterase mutants.**

523 Normalized bioluminescence production (lux/OD<sub>600</sub>) using a *Pqrr4-lux* reporter was measured in  
524 a  $\Delta 3$  *cqsR*<sup>+</sup> and the isogenic  $\Delta 3$  *cqsR*<sup>+</sup>  $\Delta vc1554$   $\Delta vca0136$  strains with and without 10 mM  
525 ethanolamine. Each figure shows a representative profile of each condition with three biological  
526 replicates. Each experiment was performed independently at least two times.

527

## 528 **Detail of chemical synthesis of HEGly and HEHEAA**

529 Unless otherwise noted, all reactions were performed in flame-dried glassware under an  
530 atmosphere of nitrogen using dried reagents and solvents. All chemicals were purchased from  
531 commercial vendors and used without further purification. Anhydrous solvents were purchased  
532 from commercial vendors. Flash chromatography was performed using standard grade silica gel  
533 60 230-400 mesh from SORBENT Technologies or was performed using a Biotage Flash  
534 Purification system equipped with Biotage silica gel or C18 columns. Analytical thin-layer  
535 chromatography was carried out using Silica G TLC plates, 200  $\mu\text{m}$  with UV<sub>254</sub> fluorescent  
536 indicator (SORBENT Technologies), and visualization was performed by staining and/or by  
537 absorbance of UV light. NMR spectra were recorded using a Varian Mercury Plus spectrometer  
538 (400 MHz for <sup>1</sup>H-NMR; 100 MHz for <sup>13</sup>C-NMR). Chemical shifts are reported in parts per million  
539 (ppm) and were calibrated according to residual protonated solvent. Mass spectroscopy data was  
540 collected using an Agilent 1100-Series LC/MSD Trap LC-MS or a Micromass Quattromicro with  
541 a Waters 2795 Separations Module LC-MS with acetonitrile containing 0.1% formic acid as the  
542 mobile phase in positive ionization mode. All final compounds were evaluated to be of greater  
543 than 90% purity by analysis of <sup>1</sup>H-NMR and <sup>13</sup>C-NMR unless otherwise indicated.

544 **2-((2-Hydroxyethyl)amino)acetic Acid, HEGly.** This compound was synthesized following the  
545 reported procedure (65) with modifications. Briefly, to a solution of ethanolamine (3.15 mL, 52.2  
546 mmol) in anhydrous THF (53mL) in a oven-dried flask was added *i*-Pr<sub>2</sub>NEt (9.4 mL, 54.0 mmol).  
547 The resulting solution was cooled to 0°C and was treated with ethyl bromoacetate (5mL,  
548 45.2mmol) dropwise. The mixture was stirred overnight with warming to room temperature and  
549 was concentrated *in vacuo* to remove solvent and was purified by silica gel flash chromatography  
550 to provide the ester, ethyl (2-hydroxyethyl)glycinate (3.5 g, 23.8 mmol, 53% yield). The ester,

551 ethyl (2-hydroxyethyl)glycinate (3.5g, 23.8 mmol) was dissolved in a solution of acetone (119mL)  
552 and water (119mL) and was treated with LiOH (4.99g, 119.01mmol) and stirred at room  
553 temperature overnight. The reaction was quenched by the addition of 119mL of 1M HCl and was  
554 concentrated to dryness *in vacuo*. The residue was purified by slow recrystallization from  
555 H<sub>2</sub>O/EtOH at 5°C to provide 2-((2-Hydroxyethyl)amino)acetic Acid, HEGly (1.10g, 9.2mmol,  
556 39% yield). Spectral data was consistent with previously reported data (65).

557 ***N*-(2-hydroxyethyl)-2-((2-hydroxyethyl)amino)acetamide, HEHEAA.** 2-((2-  
558 Hydroxyethyl)amino)acetic Acid (HEGly, 87 mg, 0.73 mmol) was dissolved in H<sub>2</sub>O (200 uL) with  
559 warming. The solution was diluted with ACN (1.5 mL) and was treated sequentially with *i*-Pr<sub>2</sub>Net  
560 (250 uL, 1.46 mmol), 2-aminoethanol (88 uL, 1.46 mmol), 1-Hydroxybenzotriazole (HOBt, 197  
561 mg, 1.46 mmol) and *N*-(3-Dimethylaminopropyl)-*N*'-ethylcarbodiimide hydrochloride (EDC, 279  
562 mg, 1.46 mmol). The resulting mixture was heated to 55 °C and was stirred overnight. The reaction  
563 mixture was concentrated to dryness and purified using C18 flash chromatography to provide *N*-  
564 (2-hydroxyethyl)-2-((2-hydroxyethyl)amino)acetamide, HEHEAA. The product HEHEAA co-  
565 eluted with 1-(3-(dimethylamino)propyl)-3-ethylurea and was characterized and used in biological  
566 studies as an inseparable ca. 1:1 mixture based on <sup>1</sup>H-NMR and <sup>13</sup>C-NMR.

567

568

569 **REFERENCES**

- 570 1. Hawver LA, Jung SA, Ng WL. 2016. Specificity and complexity in bacterial quorum-sensing  
571 systems. *FEMS Microbiol Rev* 40:738-52.
- 572 2. Suckow G, Seitz P, Blokesch M. 2011. Quorum sensing contributes to natural transformation of  
573 *Vibrio cholerae* in a species-specific manner. *J Bacteriol* 193:4914-24.
- 574 3. Lo Scudato M, Blokesch M. 2012. The regulatory network of natural competence and  
575 transformation of *Vibrio cholerae*. *PLoS Genet* 8:e1002778.
- 576 4. Hammer BK, Bassler BL. 2003. Quorum sensing controls biofilm formation in *Vibrio cholerae*.  
577 *Mol Microbiol* 50:101-4.
- 578 5. Miller MB, Skorupski K, Lenz DH, Taylor RK, Bassler BL. 2002. Parallel quorum sensing systems  
579 converge to regulate virulence in *Vibrio cholerae*. *Cell* 110:303-14.
- 580 6. Zhu J, Miller MB, Vance RE, Dziejman M, Bassler BL, Mekalanos JJ. 2002. Quorum-sensing  
581 regulators control virulence gene expression in *Vibrio cholerae*. *Proc Natl Acad Sci U S A*  
582 99:3129-34.
- 583 7. Shao Y, Bassler BL. 2014. Quorum regulatory small RNAs repress type VI secretion in *Vibrio*  
584 *cholerae*. *Mol Microbiol* 92:921-30.
- 585 8. Hawver LA, Giulietti JM, Baleja JD, Ng WL. 2016. Quorum Sensing Coordinates Cooperative  
586 Expression of Pyruvate Metabolism Genes To Maintain a Sustainable Environment for  
587 Population Stability. *MBio* 7.
- 588 9. Beyhan S, Bilecen K, Salama SR, Casper-Lindley C, Yildiz FH. 2007. Regulation of rugosity and  
589 biofilm formation in *Vibrio cholerae*: comparison of VpsT and VpsR regulons and epistasis  
590 analysis of vpsT, vpsR, and hapR. *J Bacteriol* 189:388-402.
- 591 10. Shikuma NJ, Fong JC, Odell LS, Perchuk BS, Laub MT, Yildiz FH. 2009. Overexpression of VpsS, a  
592 hybrid sensor kinase, enhances biofilm formation in *Vibrio cholerae*. *J Bacteriol* 191:5147-58.
- 593 11. Jung SA, Chapman CA, Ng WL. 2015. Quadruple quorum-sensing inputs control *Vibrio cholerae*  
594 virulence and maintain system robustness. *PLoS Pathog* 11:e1004837.
- 595 12. Rutherford ST, van Kessel JC, Shao Y, Bassler BL. 2011. AphA and LuxR/HapR reciprocally control  
596 quorum sensing in vibrios. *Genes Dev* 25:397-408.
- 597 13. Shao Y, Bassler BL. 2012. Quorum-sensing non-coding small RNAs use unique pairing regions to  
598 differentially control mRNA targets. *Mol Microbiol* 83:599-611.
- 599 14. Bardill JP, Zhao X, Hammer BK. 2011. The *Vibrio cholerae* quorum sensing response is  
600 mediated by Hfq-dependent sRNA/mRNA base pairing interactions. *Mol Microbiol* 80:1381-94.
- 601 15. Lenz DH, Mok KC, Lilley BN, Kulkarni RV, Wingreen NS, Bassler BL. 2004. The small RNA  
602 chaperone Hfq and multiple small RNAs control quorum sensing in *Vibrio harveyi* and *Vibrio*  
603 *cholerae*. *Cell* 118:69-82.
- 604 16. Higgins DA, Pomianek ME, Kraml CM, Taylor RK, Semmelhack MF, Bassler BL. 2007. The major  
605 *Vibrio cholerae* autoinducer and its role in virulence factor production. *Nature* 450:883-6.
- 606 17. Ng WL, Wei Y, Perez LJ, Cong J, Long T, Koch M, Semmelhack MF, Wingreen NS, Bassler BL. 2010.  
607 Probing bacterial transmembrane histidine kinase receptor-ligand interactions with natural and  
608 synthetic molecules. *Proc Natl Acad Sci U S A* 107:5575-80.
- 609 18. Ng WL, Perez LJ, Wei Y, Kraml C, Semmelhack MF, Bassler BL. 2011. Signal production and  
610 detection specificity in *Vibrio* CqsA/CqsS quorum-sensing systems. *Mol Microbiol* 79:1407-17.
- 611 19. Wei Y, Perez LJ, Ng WL, Semmelhack MF, Bassler BL. 2011. Mechanism of *Vibrio cholerae*  
612 Autoinducer-1 Biosynthesis. *ACS Chem Biol* 6:356-365.
- 613 20. Wei Y, Ng WL, Cong J, Bassler BL. 2012. Ligand and antagonist driven regulation of the *Vibrio*  
614 *cholerae* quorum-sensing receptor CqsS. *Mol Microbiol* 83:1095-108.

- 615 21. Surette MG, Miller MB, Bassler BL. 1999. Quorum sensing in *Escherichia coli*, *Salmonella*  
616 *typhimurium*, and *Vibrio harveyi*: a new family of genes responsible for autoinducer production.  
617 Proc Natl Acad Sci U S A 96:1639-44.
- 618 22. Schauder S, Shokat K, Surette MG, Bassler BL. 2001. The LuxS family of bacterial autoinducers:  
619 biosynthesis of a novel quorum-sensing signal molecule. Mol Microbiol 41:463-76.
- 620 23. Chen X, Schauder S, Potier N, Van Dorsselaer A, Pelczar I, Bassler BL, Hughson FM. 2002.  
621 Structural identification of a bacterial quorum-sensing signal containing boron. Nature 415:545-  
622 9.
- 623 24. Neiditch MB, Federle MJ, Miller ST, Bassler BL, Hughson FM. 2005. Regulation of LuxPQ receptor  
624 activity by the quorum-sensing signal autoinducer-2. Mol Cell 18:507-18.
- 625 25. Neiditch MB, Federle MJ, Pompeani AJ, Kelly RC, Swem DL, Jeffrey PD, Bassler BL, Hughson FM.  
626 2006. Ligand-induced asymmetry in histidine sensor kinase complex regulates quorum sensing.  
627 Cell 126:1095-108.
- 628 26. Papenfort K, Silpe JE, Schramma KR, Cong JP, Seyedsayamdost MR, Bassler BL. 2017. A *Vibrio*  
629 *cholerae* autoinducer-receptor pair that controls biofilm formation. Nat Chem Biol 13:551-557.
- 630 27. Hossain S, Heckler I, Boon EM. 2018. Discovery of a Nitric Oxide Responsive Quorum Sensing  
631 Circuit in *Vibrio cholerae*. ACS Chem Biol 13:1964-1969.
- 632 28. Upadhyay AA, Fleetwood AD, Adebali O, Finn RD, Zhulin IB. 2016. Cache Domains That are  
633 Homologous to, but Different from PAS Domains Comprise the Largest Superfamily of  
634 Extracellular Sensors in Prokaryotes. PLoS Comput Biol 12:e1004862.
- 635 29. Marchler-Bauer A, Derbyshire MK, Gonzales NR, Lu S, Chitsaz F, Geer LY, Geer RC, He J, Gwadz  
636 M, Hurwitz DI, Lanczycki CJ, Lu F, Marchler GH, Song JS, Thanki N, Wang Z, Yamashita RA, Zhang  
637 D, Zheng C, Bryant SH. 2015. CDD: NCBI's conserved domain database. Nucleic Acids Res  
638 43:D222-6.
- 639 30. Geer LY, Domrachev M, Lipman DJ, Bryant SH. 2002. CDART: protein homology by domain  
640 architecture. Genome Res 12:1619-23.
- 641 31. Mitchell AL, Attwood TK, Babbitt PC, Blum M, Bork P, Bridge A, Brown SD, Chang HY, El-Gebali S,  
642 Fraser MI, Gough J, Haft DR, Huang H, Letunic I, Lopez R, Luciani A, Madeira F, Marchler-Bauer A,  
643 Mi H, Natale DA, Necci M, Nuka G, Orengo C, Pandurangan AP, Paysan-Lafosse T, Pesseat S,  
644 Potter SC, Qureshi MA, Rawlings ND, Redaschi N, Richardson LJ, Rivoire C, Salazar GA,  
645 Sangrador-Vegas A, Sigrist CJA, Sillitoe I, Sutton GG, Thanki N, Thomas PD, Tosatto SCE, Yong SY,  
646 Finn RD. 2019. InterPro in 2019: improving coverage, classification and access to protein  
647 sequence annotations. Nucleic Acids Res 47:D351-D360.
- 648 32. Krogh A, Larsson B, von Heijne G, Sonnhammer EL. 2001. Predicting transmembrane protein  
649 topology with a hidden Markov model: application to complete genomes. J Mol Biol 305:567-80.
- 650 33. Zimmermann L, Stephens A, Nam SZ, Rau D, Kubler J, Lozajic M, Gabler F, Soding J, Lupas AN,  
651 Alva V. 2018. A Completely Reimplemented MPI Bioinformatics Toolkit with a New HHpred  
652 Server at its Core. Journal of Molecular Biology 430:2237-2243.
- 653 34. Kelley LA, Mezulis S, Yates CM, Wass MN, Sternberg MJE. 2015. The Phyre2 web portal for  
654 protein modeling, prediction and analysis. Nature Protocols 10:845-858.
- 655 35. Nishiyama S, Takahashi Y, Yamamoto K, Suzuki D, Itoh Y, Sumita K, Uchida Y, Homma M, Imada  
656 K, Kawagishi I. 2016. Identification of a *Vibrio cholerae* chemoreceptor that senses taurine and  
657 amino acids as attractants. Sci Rep 6:20866.
- 658 36. Thelin KH, Taylor RK. 1996. Toxin-coregulated pilus, but not mannose-sensitive hemagglutinin, is  
659 required for colonization by *Vibrio cholerae* O1 El Tor biotype and O139 strains. Infect Immun  
660 64:2853-6.
- 661 37. Skorupski K, Taylor RK. 1996. Positive selection vectors for allelic exchange. Gene 169:47-52.

- 662 38. Thomas J, Watve SS, Ratcliff WC, Hammer BK. 2017. Horizontal Gene Transfer of Functional Type  
663 VI Killing Genes by Natural Transformation. *MBio* 8.
- 664 39. Bose JL, Rosenberg CS, Stabb EV. 2008. Effects of luxCDABEG induction in *Vibrio fischeri*:  
665 enhancement of symbiotic colonization and conditional attenuation of growth in culture. *Arch*  
666 *Microbiol* 190:169-83.
- 667 40. McKellar JL, Minnell JJ, Gerth ML. 2015. A high-throughput screen for ligand binding reveals the  
668 specificities of three amino acid chemoreceptors from *Pseudomonas syringae* pv. *actinidiae*. *Mol*  
669 *Microbiol* 96:694-707.
- 670 41. Anantharaman V, Aravind L. 2000. Cache - a signaling domain common to animal Ca(2+)-channel  
671 subunits and a class of prokaryotic chemotaxis receptors. *Trends Biochem Sci* 25:535-7.
- 672 42. Coutinho BG, Mevers E, Schaefer AL, Pelletier DA, Harwood CS, Clardy J, Greenberg EP. 2018. A  
673 plant-responsive bacterial-signaling system senses an ethanolamine derivative. *Proc Natl Acad*  
674 *Sci U S A* 115:9785-9790.
- 675 43. Vevelstad SJ, Johansen MT, Knuutila H, Svendsen HF. 2016. Extensive dataset for oxidative  
676 degradation of ethanolamine at 55–75°C and oxygen concentrations from 6 to 98%.  
677 *International Journal of Greenhouse Gas Control* 50:158-178.
- 678 44. Ohshima N, Yamashita S, Takahashi N, Kuroishi C, Shiro Y, Takio K. 2008. *Escherichia coli*  
679 cytosolic glycerophosphodiester phosphodiesterase (UgpQ) requires Mg<sup>2+</sup>, Co<sup>2+</sup>, or Mn<sup>2+</sup> for  
680 its enzyme activity. *J Bacteriol* 190:1219-23.
- 681 45. Tommassen J, Eiglmeier K, Cole ST, Overduin P, Larson TJ, Boos W. 1991. Characterization of two  
682 genes, glpQ and ugpQ, encoding glycerophosphoryl diester phosphodiesterases of *Escherichia*  
683 *coli*. *Mol Gen Genet* 226:321-7.
- 684 46. Brewster JL, McKellar JL, Finn TJ, Newman J, Peat TS, Gerth ML. 2016. Structural basis for ligand  
685 recognition by a Cache chemosensory domain that mediates carboxylate sensing in  
686 *Pseudomonas syringae*. *Sci Rep* 6:35198.
- 687 47. Gavira JA, Ortega A, Martin-Mora D, Conejero-Muriel MT, Corral-Lugo A, Morel B, Matilla MA,  
688 Krell T. 2018. Structural Basis for Polyamine Binding at the dCACHE Domain of the McpU  
689 Chemoreceptor from *Pseudomonas putida*. *J Mol Biol* 430:1950-1963.
- 690 48. Day CJ, King RM, Shewell LK, Tram G, Najnin T, Hartley-Tassell LE, Wilson JC, Fleetwood AD,  
691 Zhulin IB, Korolik V. 2016. A direct-sensing galactose chemoreceptor recently evolved in invasive  
692 strains of *Campylobacter jejuni*. *Nat Commun* 7:13206.
- 693 49. Shrestha M, Compton KK, Mancl JM, Webb BA, Brown AM, Scharf BE, Schubot FD. 2018.  
694 Structure of the sensory domain of McpX from *Sinorhizobium meliloti*, the first known bacterial  
695 chemotactic sensor for quaternary ammonium compounds. *Biochem J* 475:3949-3962.
- 696 50. Webb BA, Karl Compton K, Castaneda Saldana R, Arapov TD, Keith Ray W, Helm RF, Scharf BE.  
697 2017. *Sinorhizobium meliloti* chemotaxis to quaternary ammonium compounds is mediated by  
698 the chemoreceptor McpX. *Mol Microbiol* 103:333-346.
- 699 51. Kendall MM, Gruber CC, Parker CT, Sperandio V. 2012. Ethanolamine controls expression of  
700 genes encoding components involved in interkingdom signaling and virulence in  
701 enterohemorrhagic *Escherichia coli* O157:H7. *MBio* 3.
- 702 52. Del Papa MF, Perego M. 2008. Ethanolamine activates a sensor histidine kinase regulating its  
703 utilization in *Enterococcus faecalis*. *J Bacteriol* 190:7147-56.
- 704 53. Martin-Mora D, Ortega A, Perez-Maldonado FJ, Krell T, Matilla MA. 2018. The activity of the C4-  
705 dicarboxylic acid chemoreceptor of *Pseudomonas aeruginosa* is controlled by chemoattractants  
706 and antagonists. *Sci Rep* 8:2102.
- 707 54. Khatri N, Khatri I, Subramanian S, Raychaudhuri S. 2012. Ethanolamine utilization in *Vibrio*  
708 *alginolyticus*. *Biol Direct* 7:45; discussion 45.



- 709 55. Penrod JT, Mace CC, Roth JR. 2004. A pH-sensitive function and phenotype: evidence that EutH  
710 facilitates diffusion of uncharged ethanolamine in *Salmonella enterica*. *J Bacteriol* 186:6885-90.
- 711 56. Garsin DA. 2010. Ethanolamine utilization in bacterial pathogens: roles and regulation. *Nat Rev*  
712 *Microbiol* 8:290-5.
- 713 57. Anderson CJ, Clark DE, Adli M, Kendall MM. 2015. Ethanolamine Signaling Promotes *Salmonella*  
714 Niche Recognition and Adaptation during Infection. *PLoS Pathog* 11:e1005278.
- 715 58. Kaval KG, Garsin DA. 2018. Ethanolamine Utilization in Bacteria. *MBio* 9.
- 716 59. Nawrocki KL, Wetzal D, Jones JB, Woods EC, McBride SM. 2018. Ethanolamine is a valuable  
717 nutrient source that impacts *Clostridium difficile* pathogenesis. *20:1419-1435*.
- 718 60. Bertin Y, Girardeau JP, Chaucheyras-Durand F, Lyan B, Pujos-Guillot E, Harel J, Martin C. 2011.  
719 Enterohaemorrhagic *Escherichia coli* gains a competitive advantage by using ethanolamine as a  
720 nitrogen source in the bovine intestinal content. *Environ Microbiol* 13:365-77.
- 721 61. Anderson CJ, Kendall MM. 2016. Location, location, location. *Salmonella* senses ethanolamine to  
722 gauge distinct host environments and coordinate gene expression. *Microb Cell* 3:89-91.
- 723 62. Thiennimitr P, Winter SE, Winter MG, Xavier MN, Tolstikov V, Huseby DL, Sterzenbach T, Tsolis  
724 RM, Roth JR, Baumler AJ. 2011. Intestinal inflammation allows *Salmonella* to use ethanolamine  
725 to compete with the microbiota. *Proc Natl Acad Sci U S A* 108:17480-5.
- 726 63. Federle MJ, Bassler BL. 2003. Interspecies communication in bacteria. *J Clin Invest* 112:1291-9.
- 727 64. Pereira CS, Thompson JA, Xavier KB. 2013. AI-2-mediated signalling in bacteria. *FEMS Microbiol*  
728 *Rev* 37:156-81.
- 729 65. Ashley JD, Stefanick JF, Schroeder VA, Suckow MA, Kiziltepe T, Bilgicer B. 2014. Liposomal  
730 bortezomib nanoparticles via boronic ester prodrug formulation for improved therapeutic  
731 efficacy in vivo. *J Med Chem* 57:5282-92.